BGSG
Volume 55
Research Paper

*Correspondence to:
Nikolaos Dimopoulos
nikos.dhmopoulos@gmail.com

DOI number:
http://dx.doi.org/10.12681/bgsg.20769
Keywords:
Central Ionian zone, calciturbidites, compression, microbreccia, microfacies analysis
Citation:
Dimopoulos N., Georgoulas E., Peridis S., Iliopoulos G., Bourli N., Antoniou P., and Zelilidis A. (2019), Re-Assessment of Depositional Conditions of Cretaceous Deposits Around the Amfilochia and Arta Areas. Bulletin Geological Society of Greece, 55, 241-259.

Publication History:
Received: 05/07/2019
Accepted: 22/11/2019
Accepted article online: 11/12/2019

The Editor wishes to thank two anonymous reviewers for their work with the scientific reviewing of the manuscript and Ms Emmanouela Konstantakopoulou for editorial assistance.

RE-ASSESSMENT OF DEPOSITIONAL CONDITIONS OF CRETACEOUS DEPOSITS AROUND THE AMFILOCHIA AND ARTA AREAS

Nikolaos Dimopoulos[1*], Eleftherios Georgoulas[1], Savvas Peridis[1], George Iliopoulos[1], Nicolina Bourli [1], Panayiota Antoniou[1], Avraam Zelilidis[1]

[1]Laboratory of Sedimentology, Department of Geology, University of Patras, 26504, Patras, Greece

nikos.dhmopoulos@gmail.com, lefterisgeorgoulasg7@gmail.com, savvasper@gmail.com, iliopoulosg@upatras.gr, geo09093@upnet.gr, panayiota97.pa@gmail.com, a.zelilidis@upatras.gr

Abstract

Sedimentological studies of the Cretaceous limestones in the central Ionian basin (Amfilochia, Arta as well as Kerasonas areas) indicate that these deposits are composed of calciturbidites interbedded with breccia-microbreccia deposits. In the Amfilochia new cross-section, with a NNW-SSE direction, the lower Cretaceous Vigla limestones and Vigla shales were outcropped for the first time. This section is directed parallel to the paleo Ionian basin axis and the fact of the lateral discontinuity of Vigla limestones and Vigla shales indicate that during the sedimentation of these two Formations there was a restriction along the paleo basin axis, probably due to synsedimentary transfer fault activity. Forty-two (42) samples from Vigla shales were analyzed for their content in $CaCO_3$ and TOC, showed that these sediments present poor to fair hydrocarbon potential. In the Arta new cross-section, with a NE-SW direction, the Upper Cretaceous Senonian deposits showed strong deformation that took place during the compressional regime that affected the Ionian basin after sedimentation. This deformation appears stronger in the western part being close to a major thrust, and thus it is possible that this deformation could be responsible for the high secondary porosity of Upper Cretaceous deposits. Microfacies analysis of these deposits showed in general that deep-sea depositional environments prevailed, nevertheless in a few cases indications for the presence of environments with a shallow character imply the existence of isolated carbonate platforms close to the studied sections. In the studied sections with an E-W direction, no lateral changes were observed in the depositional conditions within the same Formation introducing standard depositional conditions across the paleo basin.

Keywords: *Central Ionian zone, calciturbidites, compression, microbreccia, microfacies analysis*

Περίληψη

Τα αποτελέσματα των ιζηματολογικών μελετών των ασβεστολίθων του Κρητιδικού στην κεντρική Ιόνια λεκάνη (περιοχές Αμφιλοχίας, Άρτας και Κεράσωνα) προτείνουν ότι αυτές οι αποθέσεις συντίθενται από ασβεστολιθικούς τουρβιδίτες που εναλλάσσονται με αποθέσεις λατυποπαγών-μικρολατυποπαγών. Στη νέα τομή της Αμφιλοχίας, με διεύθυνση ΒΒΔ-ΝΝΑ, για πρώτη φορά έχουν επιφανειακή εμφάνιση οι αποθέσεις του κατωτέρου Κρητιδικού των ασβεστολίθων της Βίγλας και των σχιστολίθων της Βίγλας. Αυτή η τομή διευθύνεται παράλληλα με τον άξονα της Ιόνιας παλαιολεκάνης και το γεγονός της πλευρικής ασυνέχειας τόσο των ασβεστολίθων της Βίγλας όσο και σχιστολίθων της Βίγλας προτείνει ότι κατά την διάρκεια της ιζηματογένεσης των παραπάνω δύο σχηματισμών υπήρχε περιορισμός της ιζηματογένεσης κατά μήκος του άξονα της παλαιολεκάνης, προφανώς εξαιτίας της συνιζηματογενούς δράσης ρηγμάτων μετασχηματισμού. Αναλύθηκαν σαράντα δύο (42) δείγματα από τους σχιστολίθους της Βίγλας για τον προσδιορισμό του ποσοστού CaCO3 και TOC, και έδειξαν ότι τα ιζήματα αυτά έχουν φτωχό έως μέτριο δυναμικό παραγωγής υδρογονανθράκων. Στη νέα εγκάρσια τομή της Άρτας, με διεύθυνση ΒΑ-ΝΔ, στις αποθέσεις του Σενωνίου του ανωτέρου Κρητιδικού διαπιστώθηκε ισχυρή παραμόρφωση που έλαβε χώρα κατά τη διάρκεια του καθεστώτος συμπίεσης και επηρέασε την Ιόνια λεκάνη μετά την ιζηματογένεση. Αυτή η παραμόρφωση εμφανίζεται ισχυρότερη στο δυτικό τμήμα, που βρίσκεται πιο κοντά σε μια κύρια επώθηση, και έτσι προφανώς αυτή η παραμόρφωση θα μπορούσε να είναι υπεύθυνη για το υψηλό δευτερογενές πορώδες των αποθέσεων του ανωτέρου Κρητιδικού. Η μικροφασική ανάλυση των αποθέσεων αυτών έδειξε γενικά ότι επικρατούσαν κύρια συνθήκες ιζηματογένεσης βαθιάς θάλασσας, ωστόσο σε λίγες περιπτώσεις οι ενδείξεις για την παρουσία περιβαλλόντων με ρηχό χαρακτήρα υποδηλώνουν την παρουσία απομονωμένων ανθρακικών πλατφορμών κοντά στις περιοχές που μελετήθηκαν. Στις τομές που μελετήθηκαν με διεύθυνση Α-Δ, δεν παρατηρήθηκαν πλευρικές αλλαγές στις συνθήκες ιζηματογένεσης μέσα στον ίδιο σχηματισμό, προτείνοντας σταθερές συνθήκες ιζηματογένεσης εγκάρσια στον άξονα της παλαιολεκάνης.

Λέξεις-κλειδιά: *Κεντρική Ιόνιος ζώνη, ανθρακικοί τουρβιδίτες, συμπίεση, μικρολατυποπαγή, μικροφασική ανάλυση*

1. INTRODUCTION-GEOLOGICAL SETTING

Upper Cretaceous–Lower Eocene deposits of the Ionian basin (Fig. 1) are the major target in hydrocarbon exploration as they represent the main reservoir rocks. These deposits are mostly composed of calciturbidites interbedded with breccia-microbreccia deposits. According to Bourli et al., (2019a) the studied outcrops from Araxos area (internal Ionian sub-basin) showed that the breccia - microbreccia deposits are structureless, with a channelized geometry and calciturbiditic blocks internally to the channels; whereas most of the clasts were sourced from the underlying Lower Cretaceous "Vigla limestones". Moreover, microfacies analyses indicate deep-water deposits and reworked shelf deposits. The intense extensional tectonic activity in the Ionian basin during the Early Cretaceous, with synthetic and antithetic faults, produced active isolated platform margins and asymmetrical grabens. During the late Cretaceous, the uplifted margins of the grabens consisting of the Early Cretaceous "*Vigla* Formation" were eroded and got reworked. At the base of the sedimentary succession in the Ionian zone of NW Greece, there are Triassic evaporites, which are overlain by thick Mesozoic carbonates. The sediments of the Ionian zone (Fig. 2) were originally divided into three basic sequences, which correspond to three stages of evolution of the basin (Skourtsis-Coroneou, 1995; Karakitsios, 1995; 2003; 2013; Zelilidis et al., 2015).

A. Pre-rift stage (the stage before the creation of the trench): This stage is represented by the neritic (shallow-marine platform) limestones of Pantokrator, of early Jurassic age. These neritic limestones overlay, through the limestones of Foustapidima (Middle – Upper Triassic; 50-150 m thick), on the Lower-Middle Triassic evaporites, whose thickness exceeds 2000 m.

B. Syn-rift stage (the stage during the creation of the trench): A syn-rift succession was accumulated because of extensional faulting (due to the opening of the Neotethys Ocean) and evaporite halokinesis. Such tectonic activity differentiated the basin into smaller sub basins of half-graben geometry. This stage begins with the deposition of the Lower Jurassic limestones of Louros and Siniais, as lateral equivalent. These limestones signify the beginning of the subduction of the area and the onset of rifting, which is expressed by syn-sedimentary depositional prisms such as *Ammonitico rosso*, limestones with Filaments and schists with *posidonia* in the Middle and Upper Jurassic. Less complete successions with unconformities occur in the elevated parts of half-grabens.

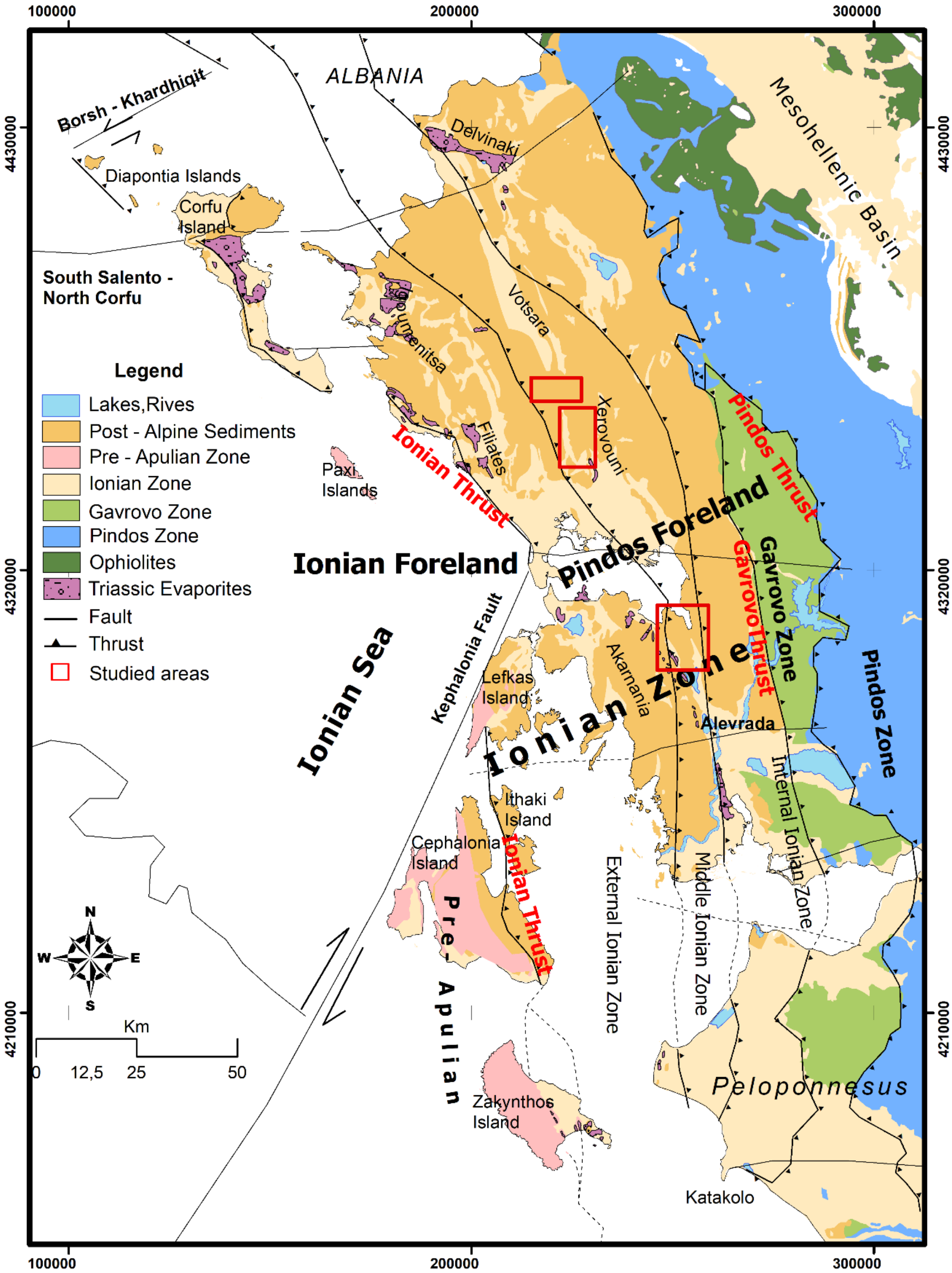

Fig. 1: Geological map of the external Hellenides in NW Greece showing the tectonostratigraphic zones: Pindos, Gavrovo, Ionian and Pre-Apulian Zones (modified from Bourli et al., 2019a). Red boxes show the studied areas.

C. Post-rift stage (the stage after the creation of the trench): This stage is determined by an unconformity at the basis of the pelagic limestones of *Vigla* in the Lower Cretaceous with a total thickness from 200m up to 600m. The "Vigla Formation" locally overlies the pre-rift succession and thickness variations indicate persistent differential subsidence. Upper Cretaceous (Senonian) limestones, rest on the Vigla Limestones. Senonian limestones consist of resedimented microbreccia and turbiditic facies and constitute the major reservoir of Ionian basin hydrocarbons. From the Upper Cretaceous (Senonian limestones) to the Upper Eocene, the pelagic sedimentation continues, and pelagic limestones are deposited in some places with characteristic thin layers supplemented by the erosion of Cretaceous limestones from both the Apulian and Gavrovo platforms. Within the Ionian Zone, the Upper Cretaceous - Eocene resedimented carbonates (calcareous turbidites and coarser breccia) are considered one of the main reservoir successions and exploration targets in western Greece.

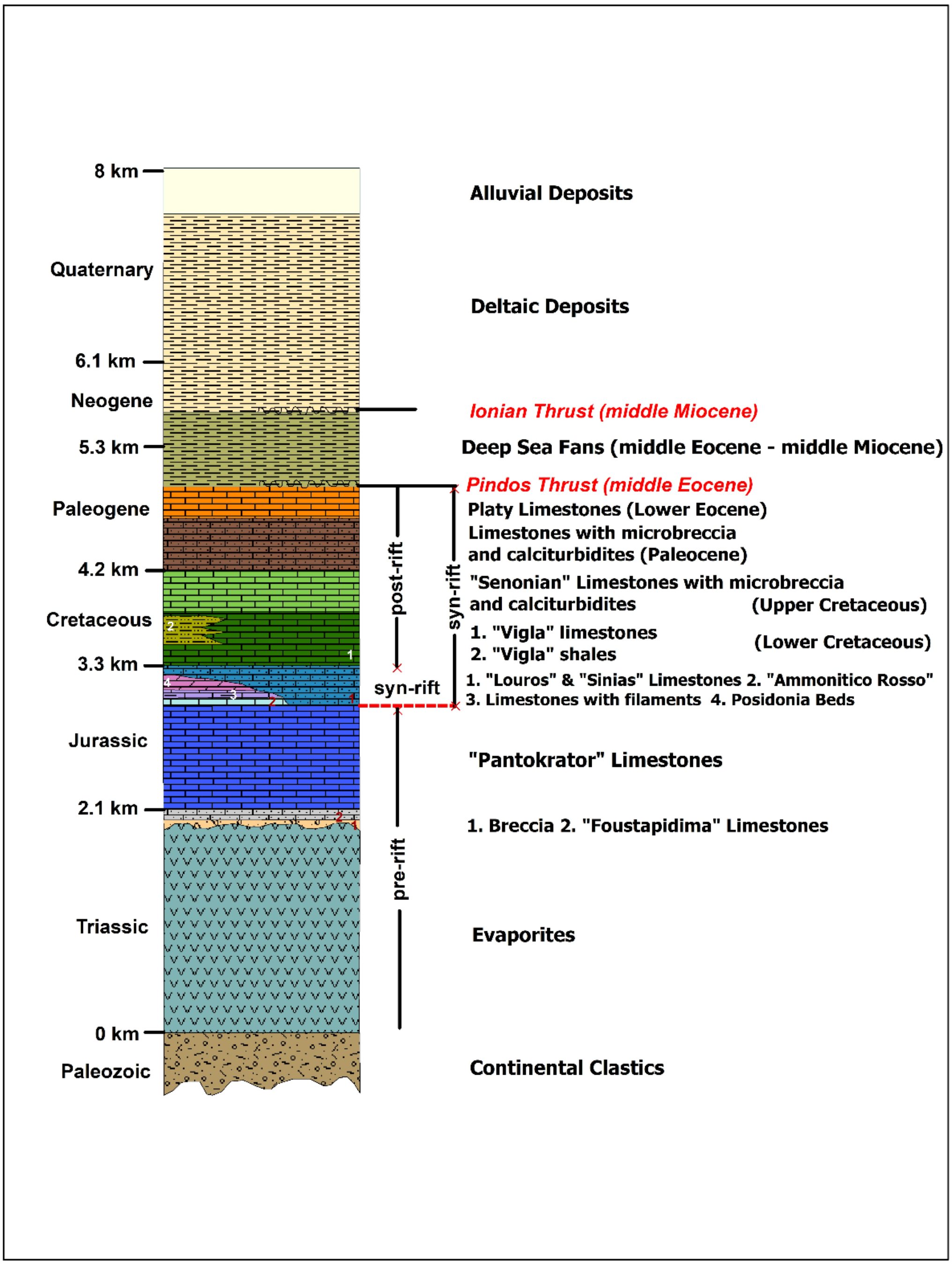

Fig. 2: Detailed lithostratigraphic column of the Ionian zone, NW Greece, according to Bourli et al. (2019a).

According to Bourli et. al. (2019a), the status about the Ionian zone has changed and the post-rift stage is included at the syn-rift. The latest and most detailed stratigraphic column that contains the actual thicknesses of the respective sequence is shown at Fig.2.

2. ANALYSIS OF THE STUDIED SECTIONS – FIELD WORK

In order to increase the knowledge for the Cretaceous evolution of the Ionian basin, two new-outcropped sections were selected in Amfilochia (with NNW-SSE direction) and Arta (with NNE-SSW direction) areas, both considered as part of the central Ionian sub-basin. Moreover, two additional sections perpendicular to the ones mentioned above were studied as well only for correlation with the previous sections. Finally, nine small sections in Kerasonas area were also studied for correlation with the two areas mentioned above.

The Amfilochia new section with NNW-SSE direction and Arta new section with a NE-SW orientation were selected parallel to the major normal and transfer faults, respectively, in order to study differences and depositional conditions influences either along or across the paleo basin axis.

The new Amfilochia section was divided into five (5) subsections (Fig. 3A). From south to north, subsection 1 is characterized by limestones whitish to grey, partly coarse – grained, medium – thick bedded to massive and brecciated with a general NW dip. The lower stratigraphic deposits correspond to the Lower Jurassic, whereas over them and in sections 2 to 5 the Lower Cretaceous "*Vigla* Formation" rest unconformably. The *Vigla* Formation consists of two different members, the lower represented by the "*Vigla* limestones" and the overlying one by the "*Vigla* shales" (Fig. 3B). Both members present a strong discontinuity along the NNW direction, with differential thickness along this direction that is mostly influenced by syn-sedimentary transfer faults. *Vigla* Formation presents internal changes in depositional thickness both in Vigla shales and in Vigla limestones. Their thickness presents a lateral wedging out, in a N-S direction, indicating depositional changes along the paleo basin axis. This axially basin changes could be related with along the basin restrictions, which could be related with the syn-sedimentary transfer fault activity. The synchronous activity of transfer faults with the major normal faults produced during the sedimentation phase paleo valleys where the Vigla shales were accumulated (compare the proposed model of Bourli et al., 2019a).

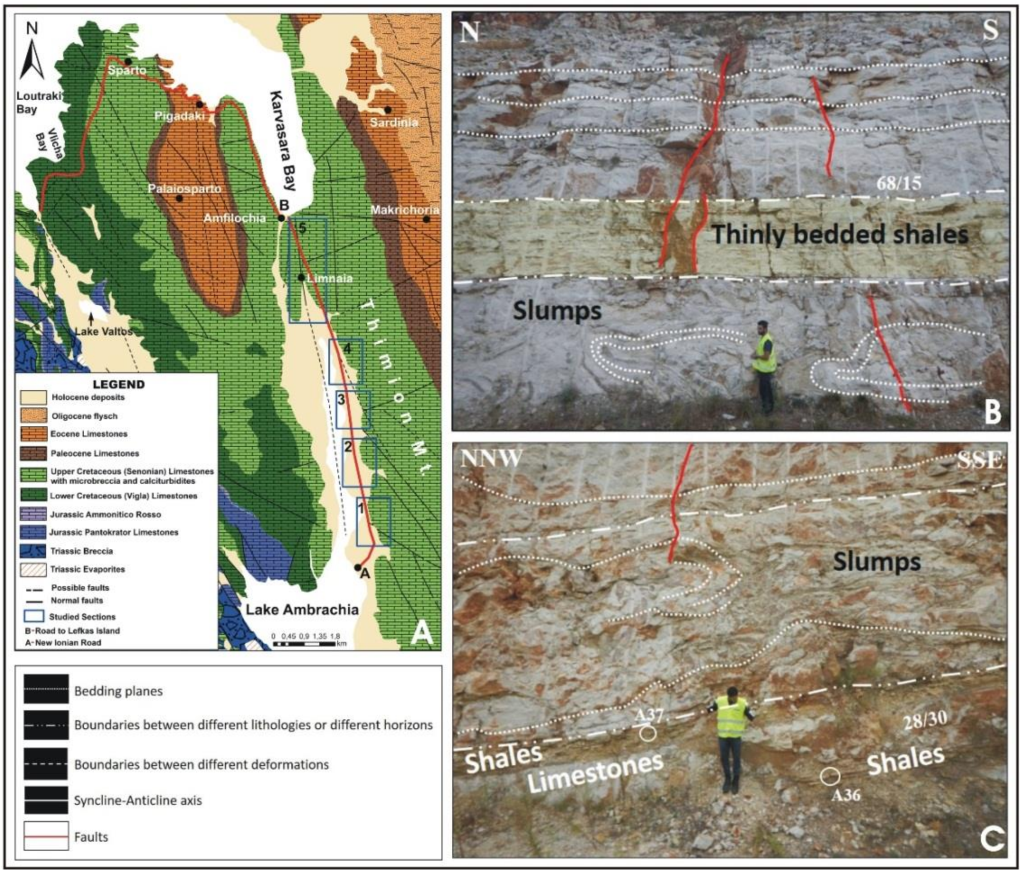

Fig. 3: A. Geological map of the studied area showing the selected areas for description and sampling, **B.** In section 2 Vigla Formation presents either a strongly deformed (slumps) horizon at the lower part, passing upwards into thinly bedded shales (yellow shadow) or thin to medium bedded limestones without any deformation in the upper part (gay shadow). This Formation is characterized by the presence of nodules within the slumped horizon, **C.** In section 5 the undeformed shales, at the base, pass upwards into a slump horizon with abundant nodules. In the upper stratigraphic part, medium-bedded limestones are observed.

In detail, the “Vigla limestones” are characterized by cycles, consisting of thin to medium-bedded limestones in rhythmic alternations with thin-bedded cherts, with a NE dip direction. The “Vigla shales” were strongly deformed either due to slumping or due to faulting (Fig. 3B, C). Slumps present an axis with E-W direction and sliding towards the west. These slumps are the result of an instability probably produced from the N-S directed normal faults (Fig. 3 B, C). These slumps are from 60 m (section 2) to 100 m (section 5) long and up to 2 m thick. Furthermore, “Vigla shales” characterized by thin to medium bedded limestones with no rhythmic alternations with thin bedded marly limestones, are dipping to the NW. Upper Cretaceous deposits (Senonian) rest unconformably over the Lower Cretaceous (Vigla Formation) sediments. The Upper

Cretaceous limestones in the Amfilochia area are up to 450 m thick. This lithology is characterized by thin to medium-bedded whitish microbreccia limestones (sections 2, 3, 4 and 5). In addition, in the uppermost part of subsection 3, laminated calcarenites (resembling to Ta, Tb and Tc Bouma sub-divisions) were recognized, that dip NW. Chert nodules occur between cycles and near the top of structureless calcarenite beds. The presence of chert nodules supports the idea of porous host deposits (Bourli et al., 2019b). In the additional section with E-W direction, along the road from Amfilochia to Lefkas Island, no changes are recognized in the depositional conditions within the same Formation.

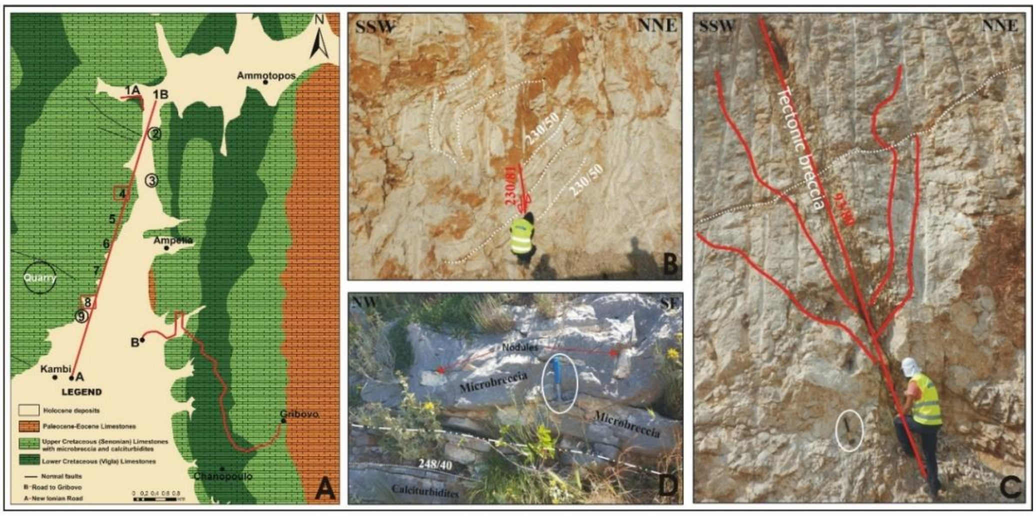

Fig. 4: A. Geological map of the studied area showing the selected areas for description and sampling, **B.** In section 4 an intense deformation was observed due to the presence of a reverse fault, with up to 30 cm displacement (see the yellow dashed line), **C.** A strike slip fault (? or transfer fault) with N-S direction, producing a positive flower structure and a 30cm thick tectonic breccia, **D.** In the road towards Gribovo village calciturbidites interbedded with microbreccia deposits with abundant either nodules or siliceous beds.

The second area is located about 10 km NW of the Arta town and is part of a continuous carbonate sequence of the Upper Cretaceous (Senonian). It was studied along the Ionian Road, with NNE-SSW direction, from the village Kambi to Ammotopos, and separated into 9 subsections (Fig. 4A).

From subsection 1 to section 9, all deposits present strong deformation, due to many reverse faults, probably branches of a major thrust fault. The fact that SW oriented deformation is stronger or increases from section 1 to section 9 indicates the presence of the major thrust west of the studied section, located very close to the studied sections. Subsection 1 is situated very close to the conjointment between a thrust fault and a strike-slip fault influencing the outcropped deposits, where several reverse faults (Fig. 4B) or strike-slip faults, with characteristic “flower structures” (Fig. 4C) were recognized. It is not clear the sense of the bed’s displacement and for this reason, these flower structures, according to Bourli et al., (2019a; figure 24), could be a) syndepositional during Cretaceous rift stage, b) or transfer faults, or c) could be flower structures of strike slip faults during compressional regime after the deposition. In the additional section on the road connecting the Ionian road with the Gribovo village, with a general E-W direction, calciturbidites were recognized over thin-bedded gray limestones of Late Cretaceous age, and a SW dip direction (Fig. 4D).

The third area of Kerasonas was studied in two (2) sections, west and east of Louros River respectively (Fig. 5A). Upper Cretaceous, Senonian, deposits consisting of medium to thick-bedded limestones are unconformably overlying Upper and Lower Jurassic medium-bedded limestones. Jurassic deposits in some places have been dolomitized. The section West of Louros River is characterized by strongly faulted outcrops, with many N-S directed normal faults and also many thrust faults with the same direction. Probably normal faults are related with the extensional regime during syn-rift stage and thrust faults with compressional regime after middle Eocene, respectively. Beds dip eastwards. Isolated outcrops of lower Jurassic *Pantokrator* limestones characterize the section East of Louros River. Furthermore, tectonic activity produced repetitive synclines and anticlines after the sedimentation and due to the compressional regime. The fact is that along the same, NNE-directed fault different deformation was observed; strong deformation is observed in the central part of the outcropped fault that slowly became weaker towards the edges of the fault, i.e. a decrease of the compressional regime influence is introduced along the fault plane. The general dip of bedding is towards SW (Fig. 5B, C).

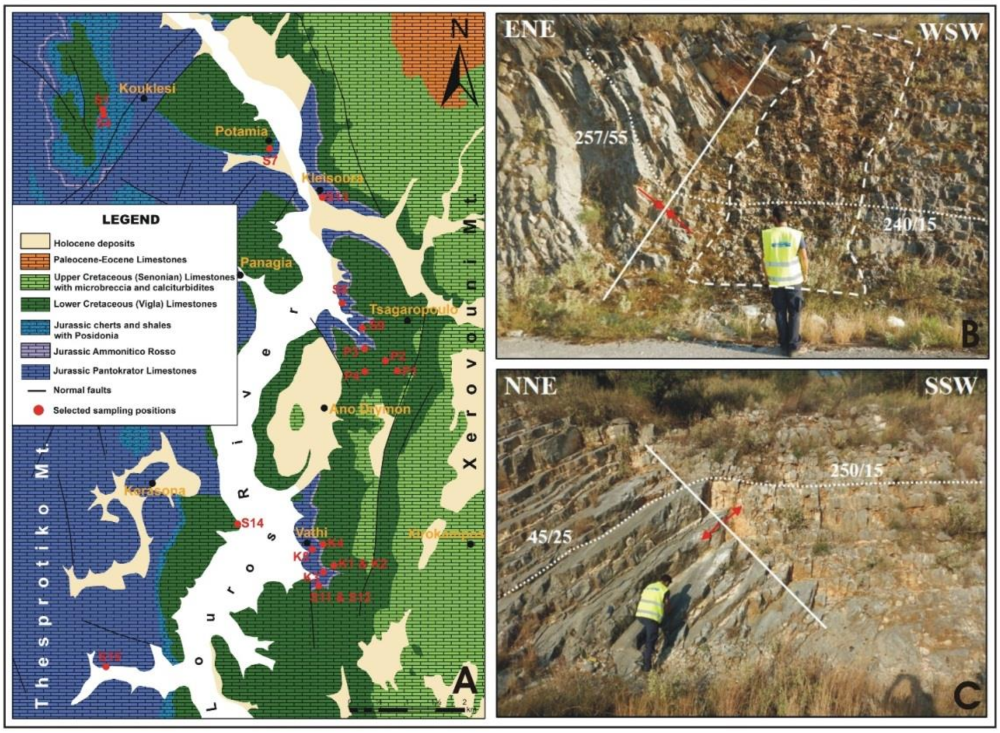

Fig. 5: A. Geological map of the studied area showing the selected areas for description and sampling points, **B.** Deformation produced a syncline within thin to medium-bedded limestones. Dashed red line marks the strongly deformed limestones that directed parallel to the syncline axis, **C.** An anticline within thin bedded limestones.

3. MICROFACIES ANALYSIS OF THIN SECTION

Microfacies analysis (Table 1) in thin sections from selected samples from Amfilochia (19 thin sections), Arta (17 thin sections) and Kerasonas (18 thin sections) showed that most of the studied deposits correspond to deep marine environments (FZ 1 & 2), some of them showed a slope to shelf environment (FZ 3 & 4) and only a few samples showed shallow water environment (see Table 2 for the exact position of selected samples). The main textural and compositional characteristics, as well as the sedimentary features of the distinguished microfacies are summarized in Table 1, corresponding to different depositional environments or facies zones (FZ: Flügel, 2010), but of course to different age deposits. Some of the used key fossils for age determination are presented in Figure 6. More specifically, the lower Cretaceous "*Vigla* limestones" were classified as packstones/wackestones with scattered planktonic foraminifera and radiolarian limestones (standard microfacies SMF 3), indicating a deep-sea basin environment (FZ 1).

Table 1. Detailed description of studied smear slides where depositional facies, lithology, fossils and the age of the studied deposits are presented (SMF= Standard Microfacies Type, FZ= Facies Zone, Pl.z.= Planktonic zone, foraminifera=forams).

No. of Samples	Facies Description	Fossils	Lithology	Stage
Amphil. sec.: 1	Pelagic wackestone with planktonic forams (SMF3). Paleoenvironment: Toe of slope (FZ3)	Planktonic forams (*Subbotina inaequispira, Globorotalia centralis, Morozovella aragonensis*)	Thin-bedded limestones with chert intervals	Eocene - [Lutetian (P1.z. 11a) - Lutetian (P1.z. 11b)]
Arta sec.: 1	Pelagic grainstone with benthic and planktonic forams (SMF2). Paleoenvironment: Deep shelf (FZ2)	Benthic & planktonic forams (*Acarinina subsphaerica, Morozovella angulata)*	Micro brecciated limestones	Paleocene - [Selandian (Pl.z. 3b) - Thanetian (Pl.z. 5a)]
Amphil. sec.: 2 Arta sec.: 2	Allochthonous bioclastic packstone to rudstone/floatstone breccia. Rudist and gastropod fragments, planktonic and benthic forams, geopetal fractures (SMF5). Paleoenvironment: Slope (FZ4)	Planktonic forams *(Globotruncana falsostuari, Siderolites calcitrapoides)* & benthic forams *(*Miliolidae, *Orbitoides media, Cuneolina sp.)*, rudist & gastropod fragments, algae	Micro brecciated limestones	Upper Cretaceous – Maastrichtian
Arta sec.: 8, Amphil. sec.: 3, Keras. sec.: 1	Two facies: 1. Pelagic wackestones with planktonic forams (SMF3). 2. Microbreccia biolithoclastic packstones to grainstones. Bioclasts, planktonic and benthic forams (SMF4). Paleoenvironment: Slope (FZ4) – Toe of slope (FZ3)	1. Benthic and planktonic forams (*Sigalitruncana sigali, Marginotruncana pseudolinneana*) 2. Benthic and planktonic forams (*Globotruncanita stuartiformis, Marginotruncana renzi)*	1. Thin-bedded limestones with chert fragments 2. Micro brecciated limestones	Upper Cretaceous – [Turonian (Pl.z. 1) – Campanian (Pl.z. 2)]
Arta sec.: 10, Amphil. sec.: 5, Keras. sec.: 15	Bioclastic pelagic packstones and wackestones that contain scattered pelagic microfossils. Paleoenvironment: Deep-sea basin (FZ1)	Radiolarians and planktonic forams (Calpionella sp.)	Vigla limestones and shales	Lower Cretaceous
Amphil. sec.: 4 Keras. sec.: 2	Paleoenvironment: (FZ9) Evaporitic/brackish platform interior – Restricted platform interior (FZ8)	Benthic forams (Miliolidae, Rotalidae) Algae	Pantokrator limestones	Lower Jurassic

Table 2. The exact position of the total seventy-six (76) selected samples from the three areas from which fifty-four (54) samples were studied for microfacies analysis.

Sample	latitude	longitude	Sample	latitude	longitude
Arta Area			**Amfilochia Area**		
D1	39 15'45.86"	20 55'42.00"	AM1	38 47'2.04"	21 11'55.71"
D2	39 15'45.15"	20 55'41.97"	AM2	38 47'2.43"	21 11'55.96"
D3	39 15'12.68"	20 55'35.93"	AM3	38 47'6.57"	21 11'54.74"
D4	39 15'03.81"	20 55'28.59"	AM4	38 47'8.00"	21 11'54.83"
D5	39 15'01.82"	20 55'27.81"	AM5	38 47'11.08"	21 11'54.45"
D6	39 15'01.44"	20 55'27.72"	AM6	38 47' 11.93"	21 11'56.28"
D7	39 14'59.40"	20 55'27.01"	AM7	38 47'14.72"	21 11'53.69"
D8	39 14'58.97"	20 55'26.95"	AM8	38 47'44.19"	21 11'48.36"
D9	39 14'55.99"	20 55'25.87"	AM9	38 47'49.78"	21 11'47.35"
D10	39 14'55.99"	20 55'25.87"	AM10	38 47'49.92"	21 11'47.89"
D11	39 14'48.03"	20 55'23.31"	AM11A	38 48'3.78"	21 11'45.23"
D12	39 14'17.72"	20 55'06.42"	AM11B	38 48'3.78"	21 11'45.23"
D13A	39 14'15.55"	20 55'05.15"	AM12	38 48'31.45"	21 11'40.47"
D13B	39 14'15.55"	20 55'05.15"	AM13	38 49'0.02"	21 11'30.55"
D14	39 13'11.56"	20 56'14.30"	AM14	38 49'9.29"	21 11'33.48"
D15	39 13'09.13"	20 56'16.16"	AM15	38 50'13.97"	21 10'58.52"
D16	39 13'15.96"	20 56'18.57"	AM16	38 50'21.93"	21 10'54.46"
D17	39 13'10.44"	20 56'21.27"	A35	38 49'27.19"	21 11'25.16"
D18	39 13'10.05"	20 56'21.58"	A38	38 49'37.05"	21 11'18.24"
D19	39 12'37.14"	20 56'33.99"	A39	38 49'38.08"	21 11'17.47"
D20	39 12'28.33"	20 56'58.50"	AL1	38 52'11.25"	21 9'37.17"
L1	39 14'37.67"	20 55'18.19"	AL2	38 52'58.65"	21 9'15.24"
L2	39 14'36.78"	20 55'17.79"	AL3	38 53'31.66"	21 8'13.34"
L3	39 14'35.30"	20 55'17.00"	AL4	38 54'1.49"	21 6'49.75"
L4	39 14'01.85"	20 54'58.25"	AL5	38 52'25.19"	21 5'11.21"
L5	39 13'59.26"	20 54'56.75"			
Kerasonas Area					
K1	39 18'11.13"	20 53'30.09"	S1	39 22'31.74"	20 50'45.39"
K2	39 18'11.39"	20 53'29.76"	S2	39 22'34.02"	20 51'28.14"
K3	39 18'10.04"	20 53'28.48"	S7	39 22'11.02"	20 52'42.87"
K4	39 18'17.50"	20 53'25.38"	S8	39 20'35.01"	20 53'48.24"
K5	39 18'22.72"	20 53'24.26"	S9	39 20'34.73"	20 53'54.79"
P1	39 19'53.52"	20 54'32.89"	S11	39 17'55.88"	20 53'16.57"
P2	39 20'14.04"	20 54'7.90"	S12	39 17'55.88"	20 53'16.57"
P3	39 20'10.39"	20 53'58.06"	S13	39 21'37.82"	20 53'18.90"
P4	39 20'3.89"	20 53'44.83"	S14	39 18'41.14"	20 52'34.91"
P5A	39 20'1.35"	20 53'10.03"	S15	39 17'12.03"	20 51'8.07"
P5B	39 20'1.35"	20 53'10.03"			

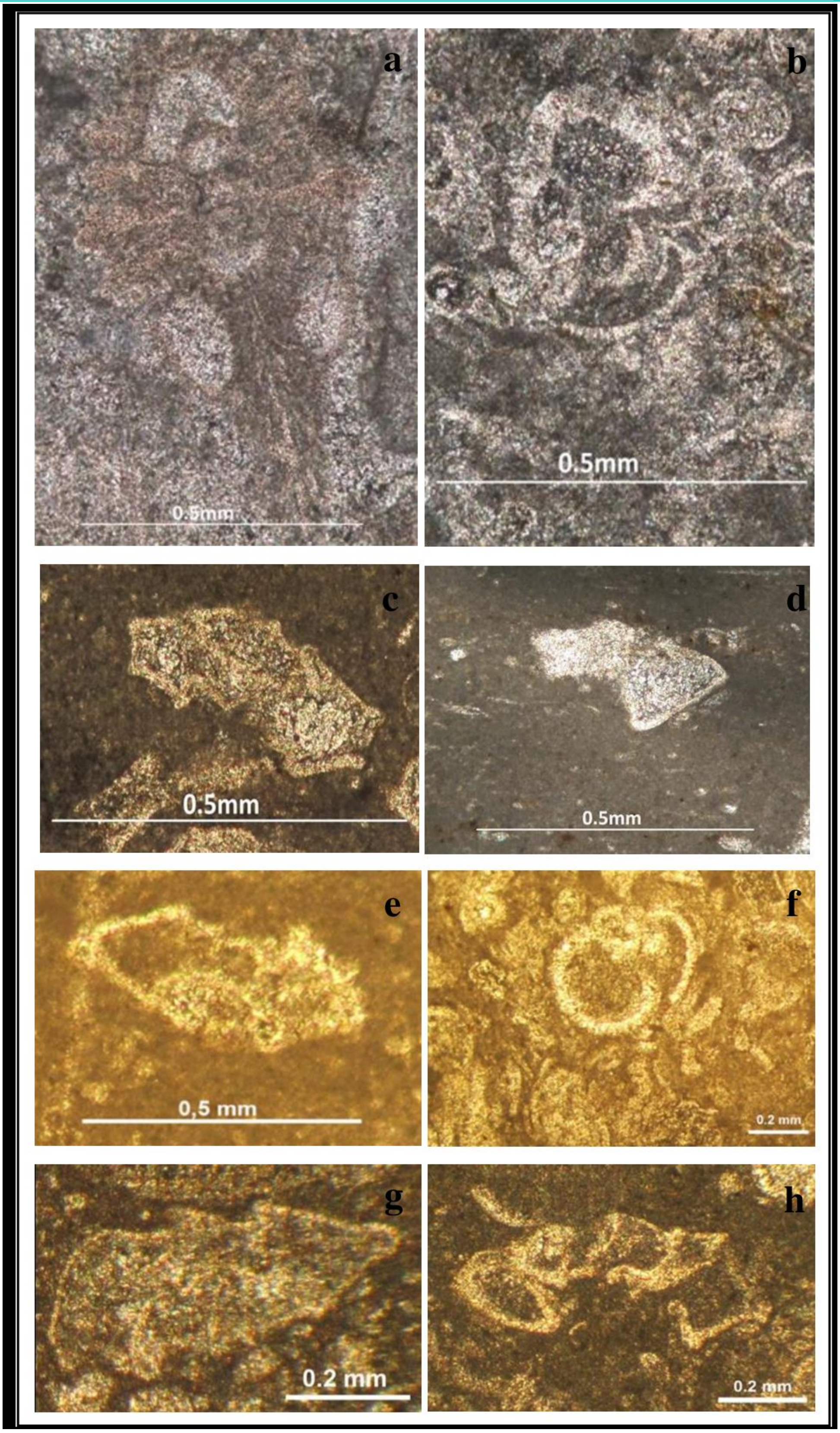

Fig. 6: Benthic and planktonic foraminifera of Amfilochia and Arta sections: **a.** Siderolites calcitrapoides, **b.** Globorotalia centralis, **c**. Marginotruncana pseudolinneana, **d.** Concavatotruncana concavata, **e.** Globotruncana stuartiformis, **f.** Acarinina subsphaerica, **g.** Globotruncanita stuarti, **h.** Sigalitruncana schneegansi.

Upper Cretaceous Senonian limestones includes pelagic wackestones with planktonic foraminifera (SMF3); microbreccia biolithoclastic packstones to grainstones (bioclasts, planktonic and benthic foraminifera (SMF4) indicating slope environment (FZ4) – toe of slope (FZ3), allochthonous bioclastic packstone to rudstone/floatstone breccia containing rudist and gastropod fragments, planktonic and benthic foraminifera, geopetal fractures (SMF5), indicating a slope environment (FZ4). Fenestral cavities and geopetal fractures in allochthonous material may indicate a source from a restricted or shallow shelf environment (FZ4) with the influence of meteoric water. The Paleocene pelagic grainstone contains planktonic and benthic foraminifera (SMF3), corresponding to a toe of slope (FZ 3). Finally, Eocene pelagic wackestones with planktonic foraminifera (SMF2), indicate a deep shelf environment (FZ3).

4. LOWER CRETACEOUS VIGLA SHALES GEOCHEMICAL ANALYSIS

In the new Ionian Road, 42 samples of clay, derived from lower Cretaceous (Vigla shales), were obtained as they were classified based on their characteristics and their age, which were analyzed for their content in $CaCO_3$ and TOC. For the determination of calcium carbonate ($CaCO_3$) content, the method for decomposition of $CaCO_3$ with CH_3COOH (acetic acid) is used (Varnavas, 1979). Quantitative determination of organic carbon (TOC) in the sample based on the oxidation of the organic carbon content in the samples was performed with the titration method (Gaudette et al, 1974). It is obvious that laboratory analyses aimed to the determination of organic matter and calcium carbonate refer to a very small part of the studied stratigraphic column in order to interpret the sedimentation conditions of these sediments.

Calcium carbonate analysis showed that the average number of samples in calcium carbonate was 24.40%. Samples A31 and A42 show the highest percentages in calcium carbonate, with values of 68.51% and 68.15%, respectively. In contrast, the A20 and A17a samples show the lowest percentages in calcium carbonate by 0.8% and 2.14% respectively. There is a very huge range in the percentage of calcium carbonate. More specifically, it has been observed that in section 1 (from sample A1 to A23) the samples are very poor in calcium carbonate, whereas in section 5 (from A30 to A42) the samples are very rich in calcium carbonate. Organic carbon analysis showed that the average of the samples was 0.54%, with fair to good hydrocarbon potential. However, there are samples that are either close to 1% (A14b, A17b, A18b, A22, A41 and A42) or more than 1% (A16b, A37 and A38) with very good hydrocarbon potential. A more detailed study is necessary in order to recognize the kerogen type for the prediction of petroleum or gas hydrocarbons productivity (Fig. 7).

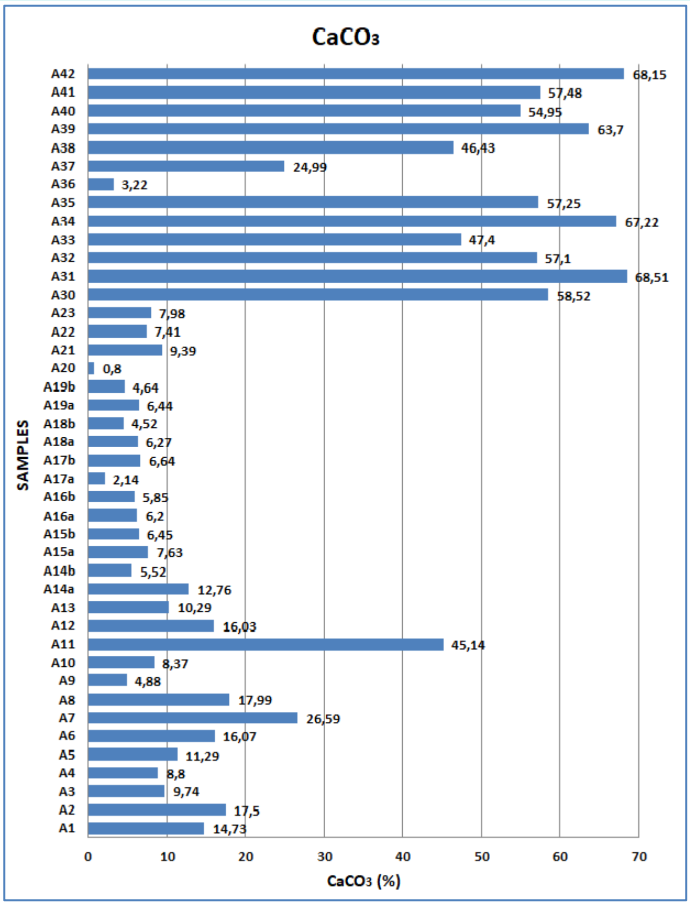
CaCO3
A42 68,15
A41 57,48
A40 54,95
A39 63,7
A38 46,43
A37 24,99
A36 3,22
A35 57,25
A34 67,22
A33 47,4
A32 57,1
A31 68,51
A30 58,52
A23 7,98
A22 7,41
A21 9,39
A20 0,8
A19b 4,64
A19a 6,44
A18b 4,52
A18a 6,27
A17b 6,64
A17a 2,14
A16b 5,85
A16a 6,2
A15b 6,45
A15a 7,63
A14b 5,52
A14a 12,76
A13 10,29
A12 16,03
A11 45,14
A10 8,37
A9 4,88
A8 17,99
A7 26,59
A6 16,07
A5 11,29
A4 8,8
A3 9,74
A2 17,5
A1 14,73
SAMPLES
0 10 20 30 40 50 60 70
CaCO3 (%)

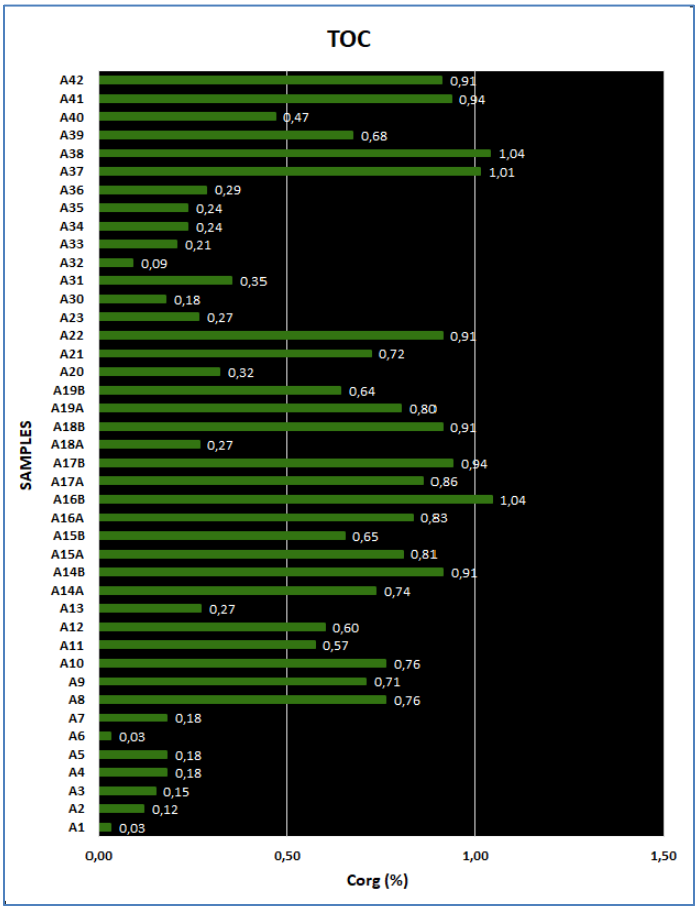
TOC
A42 0,91
A41 0,94
A40 0,47
A39 0,68
A38 1,04
A37 1,01
A36 0,29
A35 0,24
A34 0,24
A33 0,21
A32 0,09
A31 0,35
A30 0,18
A23 0,27
A22 0,91
A21 0,72
A20 0,32
A19B 0,64
A19A 0,80
A18B 0,91
A18A 0,27
A17B 0,94
A17A 0,86
A16B 1,04
A16A 0,83
A15B 0,65
A15A 0,81
A14B 0,91
A14A 0,74
A13 0,27
A12 0,60
A11 0,57
A10 0,76
A9 0,71
A8 0,76
A7 0,18
A6 0,03
A5 0,18
A4 0,18
A3 0,15
A2 0,12
A1 0,03
SAMPLES
0,00 0,50 1,00 1,50
Corg (%)

Fig. 7: Bar diagrams showing the content percent (%) of the studied samples in calcium carbonate as well as organic material. For sample location, see Table 2. In detail: Samples A1 to A6 are from the same section with AM3, samples A7 to A11 are from the same section with AM5, samples A12 to A23 are from the same section with AM6, samples A30 and A31 are from the same section, samples A32 to A35 are from the same section, and samples A36 and A37 are also from the same section.

In the lower and middle stratigraphic levels, the samples A8, A9, A10, A12, A14a, A14b, A15a, A15b, A16a, A16b, A17a, A17b, A18b, A19a, A19b, A21 and A22, showed high organic matter content which is accompanied by low calcium carbonate content, indicating more anoxic conditions. In the upper stratigraphic levels, the samples A30, A31, A32, A33, A34, A35 and A40, showed a decrease in organic matter, which is accompanied by an increase of calcium carbonate, suggesting oxidative conditions (Fig. 8).

In some cases (samples A37-A42), that both TOC and carbonate carbon are high, they could be related with very high TOC contents in oxidative conditions that destroyed a high percentage of the original TOC, but still remained high.

5. DISCUSSION AND CONCLUSIONS

The studied areas showed syn-sedimentary influenced conditions during extensional regime; whereas their outcropping was due to the after sedimentation compressional regime. Therefore, the strong deformations with reverse faults as well as synclines and anticlines were the result of the compressional regime.

In Amfilochia a new cross-section, with a N-S direction was studied. The new cuts evidenced the presence not only of the Upper Cretaceous deposits but also the presence of the Lower Jurassic *Pantokrator* limestones (section 1) which are overlaid by Lower Cretaceous *Vigla* shales or *Vigla* limestones (section 2, 3, 4, 5). Based on bedding, outcropping as well as the microfacies analysis it is suggested that the older stratigraphic units are located in the southern part of the studied sections or southwards, in section 1. According to the microfacies analysis, the lower stratigraphic deposits were accumulated in a very shallow environment and belong to the lower Jurassic *Pantokrator* limestones.

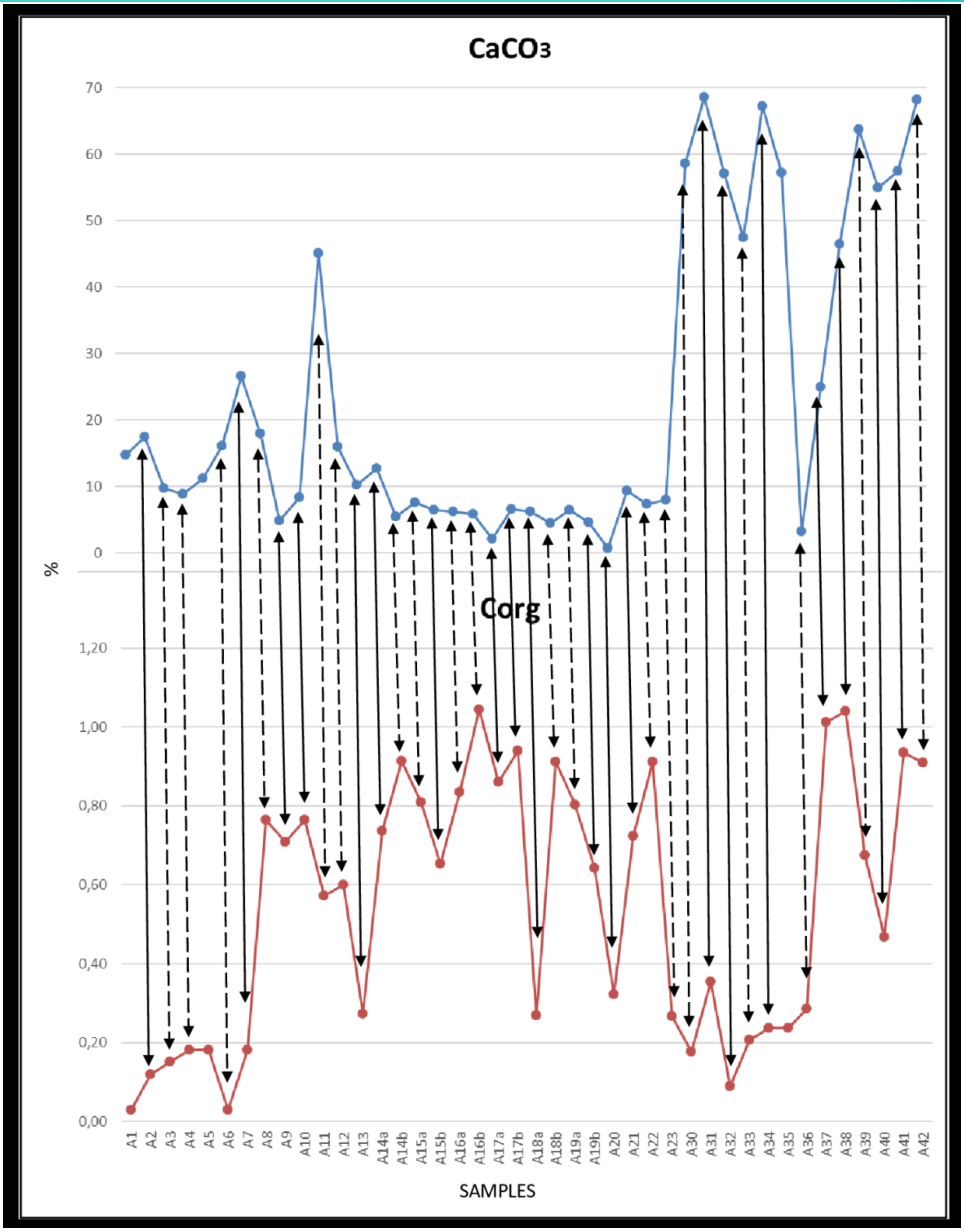

Fig. 8: Diagram showing the relationship between organic carbon (TOC) and calcium carbonate ($CaCO_3$) of the samples in Amfilochia new cross section. The dashed line shows the negative correlation between calcium carbonate and organic material, while the continuous line shows the positive correlation between calcium carbonate and organic material. For the sample position, see figure 7 caption.

In the northern part of the studied section, of the new road, Lower Cretaceous *Vigla* limestones and *Vigla* shales were outcropped. In some places, the Upper Cretaceous Senonian limestones rest unconformably over the *Vigla* shales; whereas in other places they rest unconformably over the *Vigla* limestones.

Additionally, the results from the E-W directed section, along the road from Amfilochia to Lefkas, with no depositional changes across the paleo basin, indicate no influence or any change due to syn-sedimentary fault activity. Moreover, TOC results of the Lower Cretaceous *Vigla* shales in Amfilochia new cross section showed more anoxic conditions at the lower stratigraphic levels and the content of organic matter introduce the possibility of being source rocks, with fair to good hydrocarbon potential. Additional work is needed to reconstruct the depositional conditions and to find the kerogen type and the maturity conditions. In the Arta new cross-section, with a NNE-SSW direction, the Upper Cretaceous Senonian deposits showed strong deformation that took place during the compressional regime that affected the Ionian basin after the carbonate sedimentation. Variations in sedimentary conditions, according to microfacies analysis, suggest that the above thrust faults may have acted as normal faults during sedimentation, thus affecting sedimentation conditions. In the additional, E-W directed, section there was no changes in the depositional conditions during sedimentation. So, in both areas, Arta and Amfilochia a change in depositional conditions along the paleo basin axis is suggested whereas no changes occurred across the basin axis. In the studied Kerasonas area, the main result is that the strong deformation is owed to the compressional regime that affected the Ionian basin after sedimentation. Because of this, repetitive synclines and anticlines were formed, with a decrease of this deformation in an NNE direction. Microfacies analysis showed that most of the samples belong to a deep-sea basin environment; whereas only a few samples showed a shallower water environment, which could be located on the margins of the basin, or they could be formed in isolated platforms.

In general, the upper Cretaceous Senonian limestones are characterized by microbreccia, calciturbidites and slumps, as recognized in other areas (Bourli et al., 2019a). In total, microfacies analysis from all the studied sections, showed in general a deep-sea environment of sedimentation, with a few exceptions that indicate a shallower environment character, introducing the possibility for the existence of platforms, close to the studied sections.

6. ACKNOWLEDGMENTS

Nicolina Bourli is a PhD student and she was financially supported by the "Andreas Mentzelopoulos Scholarships for the University of Patras". We would like to thank the Journal Editor Dr. A. Ganas and the two anonymous reviewers for their valuable and constructive comments and suggestions on the manuscript.

7. REFERENCES

Bourli, N., Pantopoulos, G., Maravelis, A.G., Zoumpoulis, E., Iliopoulos, G., Pomoni-Papaioannou, F., Kostopoulou, S., Zelilidis, A., 2019a. Late Cretaceous to Early Eocene geological history of the eastern Ionian Basin, southwestern Greece: An integrated sedimentological and bed thickness statistics analysis. *Cretaceous Research*, 98, 47-71.

Bourli, N., Kokkaliari, M., Iliopoulos, I., Pe-Piper, G., Piper, D.J.W., Maravelis, A.G., Zelilidis, A., 2019b. Mineralogy of siliceous concretions, Cretaceous of Ionian zone, western Greece: implication for diagenesis and porosity. *Marine and Petroleum Geology*, 105, 45-63.

Flügel, E., 2010. Microfacies Analysis of Carbonate Rocks. Springer Verlag, Berlin, 745 p.

Gaudette, H.E., Flight, W.R., Toner, L., & Folger, D.W., 1974. An inexpensive titration method for the determination of organic carbon in recent sediments. *Jour. Sed. Petr.*, 44, 249-253.

Karakitsios, V., 1995. The influence of pre-existing structure and halokinesis on organic matter preservation and thrust system evolution in the Ionian basin, northwestern Greece. *AAPG Bulletin*, 79, 960-980.

Karakitsios, V., 2003. Evolution and Petroleum Potential of the Ionian Basin (northwest Greece). AAPG International Conference, Sept. 21-24, Barcelona.

Karakitsios, V., 2013. Western Greece and Ionian Petroleum systems. *AAPG Bulletin* 97 (9), 1567–1595.

Skourtsis-Coroneou, V., Solacious, N., Constantinidis, I., 1995. Cretaceous stratigraphy of the Ionian Zone, Hellenides, western Greece. *Cretaceous Research*, 16, 539-558.

Varnavas, S.P., 1979. Geochemistry of sediments from the eastern Pacific. Ph. D. Thesis University London, 431 pp.

Zelilidis, A., Maravelis, A.G., Tserolas, P., Konstantopoulos, P.A., 2015. An overview of the petroleum systems in the Ionian Zone, onshore NW Greece and Albania. *Journal of Petroleum Geology*, 38 (3), 331-348.